

Advanced Forming Analysis for Bar and Wire Rod with Finite Element Method

Osamu KADA*¹
Hidekazu YANAGI*²

Masahiro TODA*¹

Abstract

Finite Element Method (FEM) comes to be used widely to optimize forging process effectively. 2D-FEM was used mainly around 10 years ago. But now, computer ability is rapidly developed, 3D-FEM comes to be used rapidly. In this paper, it is introduced that 3D-FEM is applied to some three-dimensional shape parts. And it is introduced that 2D-FEM is applied to multi-stage drawings for wire.

1. Introduction

Many mechanical parts, including automotive parts, are forged from bar and wire rods. Since there are many different shapes of mechanical parts, various types of forging steels are used. Therefore, there is a very high number of combinations using the two. Today, instead of studying them experimentally, positive efforts are being made to optimize the forging process by using the Finite Element Method (FEM) with the aim of eliminating the need for prototypes and shortening the creation process time. Nippon Steel Corporation has been tackling the FEM analysis of forging of bar and wire rods for more than 20 years.

Up until about 10 years ago, the practical analytical code available on the market had been mostly for two-dimensional FEM analysis, such as the analysis of axis symmetry. With the dramatic improvement in computer capacity in recent years, three-dimensional FEM analysis has rapidly become widespread¹⁾. As a result, it has become possible to directly analyze the shapes of actual parts which could formerly be analyzed only as two-dimensional models (axis symmetry or plane strain).

This paper introduces examples of FEM analysis of three dimensional forged parts. In addition, as an example of application of FEM analysis to a complicated manufacturing process, an FEM analysis of multi-stage drawing is discussed.

2. Forging Simulation System

The authors have developed a forging simulation system²⁾ which incorporates the company's databases on the material properties of forging steel in FEM analysis as the accuracy of FEM analysis is

determined largely by the material properties data used for the analysis. The outline of the system is shown in Fig. 1. The databases on the material properties of forging steel contain: (1) data on the flow stress curve of steel for cold forging, (2) data on the ductile fracture of steel for cold forging and (3) data on the flow stress curve of steel for hot forging³⁾. The steel material conditions (chemical composition, heat treatment conditions, forging temperature, etc.) that are

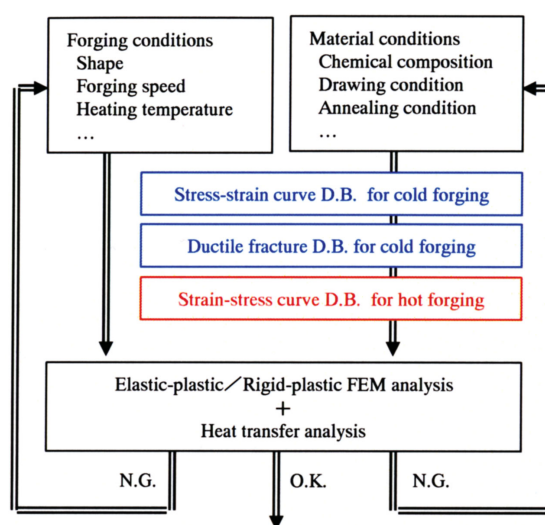


Fig. 1 Forging simulation system

*¹ Steel Research Laboratories

*² Matsubishi Metal Industry Co., Ltd.

input are converted into material constants and used for FEM analysis. For two-dimensional models, such as those of axis symmetry, the 2D rigid-plastic FEM developed by ourself is used. For three-dimensional models, 3D FEM analysis code available on the market is used. In either case, sufficient accuracy of the analysis is achieved by utilizing the databases on the material properties of forging steel.

Thanks to the remarkable improvement in computer capacity in recent years, the time taken for computing in three-dimensional FEM analysis has been significantly reduced. However, in three-dimensional FEM analysis, preparing the input data takes considerable time because the dies are of complicated shape. Therefore, it is desirable to use a two-dimensional model as much as possible. With the complication of shapes of forged parts in recent years, however, problems which cannot be solved by two-dimensional analysis are increasing in number. An example of this is given below.

3. Estimation of Flower-petal Shape and Cracking of Flanged Head Bolt

The head of a flanged head bolt is hexagonal in shape. However, when it comes to estimating the forging load, for example, it has been common practice to approximate the head shape by a cylinder having the same cross-sectional area so that two-dimensional axis-symmetric FEM analysis can be applied. As a flower-petal shaped deformation of the flange occurred, whereby the flange diameter across opposite sides becomes larger than that across the opposite angles, the deformation was analyzed by three-dimensional FEM.

A flanged head bolt of the shape shown in Fig. 2 was subjected to three-dimensional FEM analysis. Fig. 3 shows the condition of development of the deformation. The left side shows the deformation of the cross section across the opposite sides (Fig. 2-A), and the right side shows the deformation of the cross section across the opposite angles (Fig. 2-B). At the opposite sides, where the volume of the hexagonal part is smaller than at the opposite angles, the material

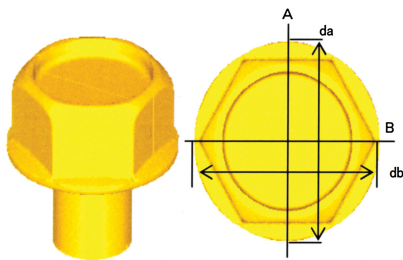


Fig. 2 Shape of flanged head bolt

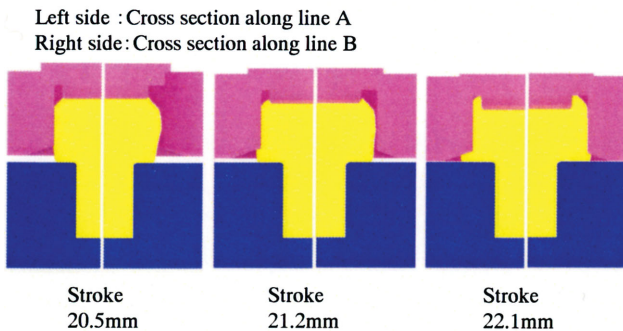


Fig. 3 Change of die filling in flanged head bolt

fills the dies earlier and flows toward the flange. At the opposite angles, by contrast, the material flow toward the flange is delayed. As a result of this, the flange diameter across the opposite sides becomes larger. Let us define the ratio of the flange diameter across the opposite sides to the flange diameter across the opposite angles as the degree of flower petal shape (da/db). Then, with the progress of the processing, its da/db increases as shown in Fig. 4. In the case of the flanged head bolt under consideration, the da/db is 1.006 with the standard punch stroke of 22.1 mm. When the punch stroke is increased by 0.3 mm, the da/db becomes 1.015. Thus, it can be seen that even with a slight change in punch stroke the degree of flower petal shape varies significantly.

For example, when the material is softened in order to prolong the die life, the softening reduces the forging load, thereby decreasing the amounts of elastic deformation of the dies and forging machine. In this case, the amount of elastic deformation decreases as the amount of processing of the material increases if the forging machine stroke is not adjusted. As a result, a flower petal shaped deformation occurs. It is considered that a flower petal shaped deformation will also occur when the material is heavier than the prescribed weight.

To predict forging crack, the authors used the generalized Cockcroft-Latham formula expressed by the following equation (1) that is introduced to general-purpose software as an equation for evaluating ductile fracture.

$$D_f = \int \frac{\sigma^*}{\sigma} d\epsilon \quad (1)$$

D_f : Damage factor

σ^* : Maximum tensile principal stress

σ : Equivalent stress

$d\epsilon$: Equivalent strain increment

Fig. 5 shows the damage factor distribution in a flanged head bolt. The critical upsetting ratio of the material is assumed to be 60%. Red indicates the portion that is very likely to crack. Looking at the flange, the opposite sides show a large damage factor. This is considered to correspond to the fact that the flange diameter across the opposite sides becomes larger than that across the opposite angles. Concerning the recess too, the opposite sides and angles that are not in contact with the dies show large damage factors. Thus, three-dimensional FEM analysis is revealing information which could not

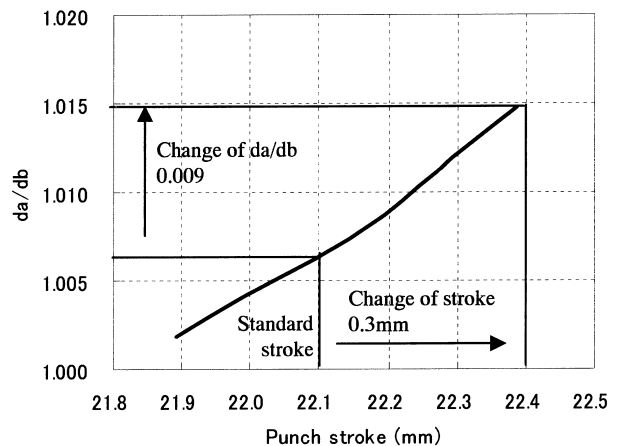


Fig. 4 Relation between punch stroke and da/db

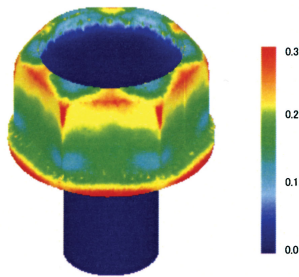


Fig. 5 Damage factor distribution in flanged head bolt

be found by using the conventional two-dimensional axis-symmetric FEM analysis. With a flanged head bolt of the shape shown above, it was estimated that the bolt could be formed without cracking as long as the critical upsetting ratio was 65% or more.

4. Prediction of Forging Crack in non-axis symmetric parts with Backward Extrusion

With the advances in forging technology and forging steel, even non-axis symmetric parts, such as the outer race for constant velocity joint, which were formerly fabricated by hot forging, have come to be increasingly manufactured by cold forging⁴⁾. Here, an example of prediction of cold forging crack in and around the inner bottom of the thick-walled portion of a deformed back-extruded part as shown in Fig. 6 is introduced.

To evaluate ductile fracture, Oyane's formula⁵⁾ expressed by the following equation (2) was applied. While in the generalized Cockcroft-Latham formula (Equation 1) the maximum principal stress is the only stress that is handled, Oyane's formula (Equation 2) evaluates the axial, radial and hoop stresses via mean stress σ_m . Therefore, it was considered that the latter would permit evaluating complicated stress conditions in parts having a complicated shape more accurately. When the Index of Oyane's Integral (I.O.I)—the integral value in Equation 2 divided by material constant C that indicates the material forgeability—exceeds 1, it is judged that the forgeability limit of the material is reached and a crack occurs.

$$\int \left(1 + \frac{1}{a} \sigma_m^{-m} \right) d\epsilon = C \quad (2)$$

a, C : Material constants

σ_m : Mean stress

ϵ : Equivalent strain

$d\epsilon$: Equivalent strain increment

Fig. 7 shows the I.O.I distribution obtained by axis-symmetric

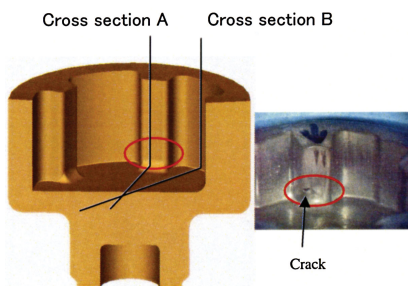


Fig. 6 Parts shape and cracking position

FEM analysis of the cross-section shapes of the thick-walled and thin-walled portions. The I.O.I in the area of the inner bottom is 0.1 or less, suggesting that cracking would not occur. This result does not indicate the accrual condition. Fig. 8 shows the I.O.I distribution obtained by three-dimensional FEM analysis. It can be seen that the I.O.I at the inner bottom of the thick-walled portion is about 0.8. This is considered to have occurred due to shrinkage on the outside of the thick-walled portion (see Fig. 9).

In the forging process, as the material is in contact with the dies, the interior of the material is subject to compressive stress, which limits cracks occurring. It is considered, however, that the occurrence of shrinkage caused the material to separate from the dies and crack under a tensile stress. When backward extrusion is applied to a part having a thin-walled bottom with a small reduction of area, shrinkage can occur at the outer bottom. However, in the two-dimensional axis-symmetric FEM analysis shown in Fig. 7, no shrink-

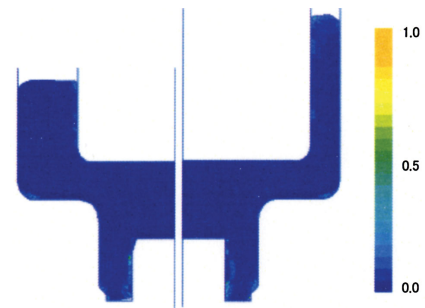


Fig. 7 I.O.I distribution obtained by 2D-FEM

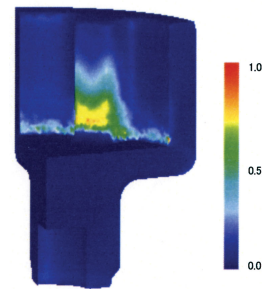


Fig. 8 I.O.I distribution obtained by 3D-FEM

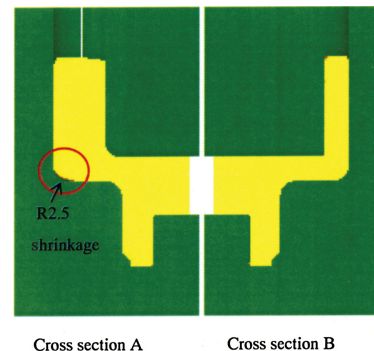


Fig. 9 Shrinkage on the outside parts (R2.5)

age was observed. It is considered that the occurrence of shrinkage is also influenced by the circumferential material flow from the thin-walled portion having a large reduction of area to the thick-walled portion. Thus, it may be said that the prediction of cracking in the part under consideration is possible only by three-dimensional FEM analysis.

In the present analysis, the I.O.I was not more than 1. Therefore, it was judged that cracking would not occur, although the part was subject to severe forming. Cracking did occur however and the authors, therefore, studied the change in material temperature due to the heat generation under plastic deformation. Fig. 10 shows the material temperature distribution obtained by three-dimensional FEM with thermal analysis. It was predicted that the material temperature at the inner bottom would rise to 300 or higher due to the forming heat. At such a high region of temperature, some steel grades become blue-shortness and decline in ductility. Cracking was therefore considered to have occurred due to a decline in ductility and an increase in tensile stress caused by shrinkage.

To restrain the occurrence of crack, an effective measure is to reduce the tensile stress as indicated by Equation 2. As means of reducing the tensile stress, increasing the radius of the punch bottom, applying a back-pressure to the backward-extruded part, etc. can be considered as an option. However, depending on the specifications of the part and forging machine, it is not always possible to adopt the above methods. Here, the authors changed the die corner radius and discussed ways of restraining the occurrence of shrinkage and thereby reducing the tensile stress. Fig. 11 shows an enlarged view of thick-walled portion of the part under consideration. By reducing the die corner radius, the area of contact between the back-extruded material and the die can be increased. This increases the frictional resistance between the material and the die, thereby re-

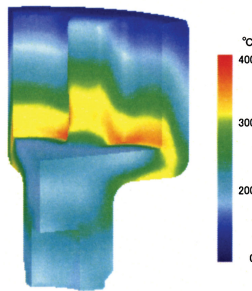


Fig. 10 Temperature distribution obtained by 3D-FEM with thermal analysis

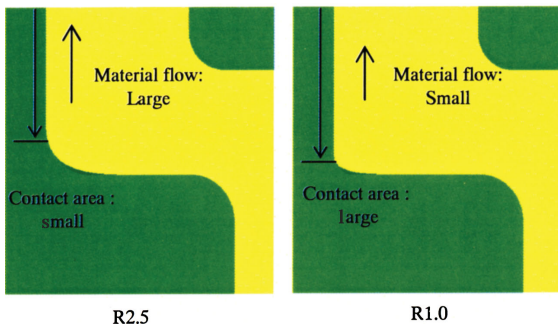


Fig. 11 Reducing shrinkage by change R of outside die

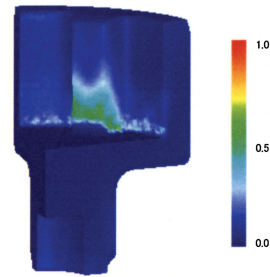


Fig. 12 I.O.I distribution obtained by 3D-FEM (R1.0)

straining the upward flow of the material. Fig. 12 shows the I.O.I distribution when the die corner radius was changed from 2.5 to 1.0. The maximum value of I.O.I decreased from 0.8 to 0.6. Parts were trial-forged by using dies whose corner radius was reduced. The rate of occurrence of cracking dramatically decreased, to 1/5. Thus, the above measure proved effective.

5. Application to Multistage Drawing

There is a growing demand for higher-strength bars and wire rods, such as steel tire cords, PWS® and saw wires. As the material strength is increased, the breaking of wire and the heat generation during drawing and other problems become more noticeable. Intuition and experience were considered to be necessary in the design process in this particular field. Recently, however, it has become essential to design a process more efficiently by applying FEM analysis from the standpoint of shortening the lead time, etc. Concerning FEM analysis of the heat generation during wire drawing, there are a good number of examples^{6,7)}, including the analysis by Kemp et al.⁸⁾. With respect to the breaking of wire during drawing, there is an analysis report of Komori et al.⁹⁾ using rigid-plastic FEM. In any case, they used their own FEM program and analyzed only a few stages of drawing. Examples of FEM analysis of drawing passes over 20 stages, such as for steel tire cords, are virtually nonexistent. The authors are tackling analysis of multistage drawing using general-purpose FEM code.

The concept of analysis of multistage drawing is shown in Fig. 13. Following the first drawing analysis, multistage drawing is analyzed by using the strain distribution in the deformed part in a steady state as the strain distribution in the material in the next pass. Fig. 14 shows an example of the analysis of 24-stage drawing of steel tire cord. In the analysis, the general-purpose FEM code “MARC” was used. The analysis mode was an axis-symmetric, elastic-plastic analysis. The coefficient of friction, μ , was assumed to be 0.07. Fig. 14 shows the equivalent strain distribution in material cross section over 24 stages. The horizontal axis represents the distance from the center, with the distance being dimensionless as it was divided by the material diameter. Fig. 15 shows the strain distribution at the 15th stage of drawing. The maximum strain is observed at a point a little beneath the surface. The mode of strain distribution differs according to the reduction in area and the half die angle. In this particular example of ours, the mode of strain distribution does not change much from the initial stage of drawing.

Fig. 16 shows the temperature history of the material center and surface, respectively, at the 15th stage. The drawing speed was about 300 m/min and the heat transfer coefficient was 10kW/m²K (with water cooling). It can be seen that due to the friction loss with the dies, the material surface temperature rises as a result of heat generation. Fig. 17 shows the temperature distribution at the 15th stage.

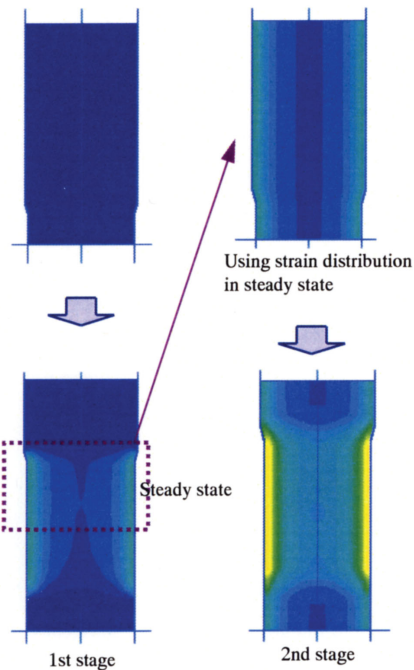


Fig. 13 Analysis method for multi stage drawing

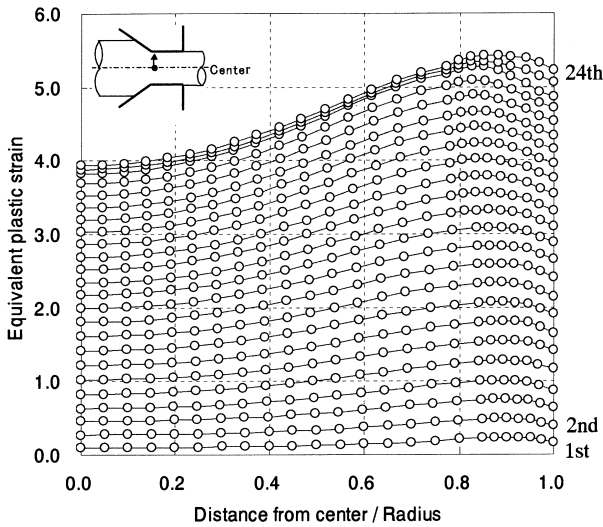


Fig. 14 Equivalent plastic strain distribution in multi stage drawing

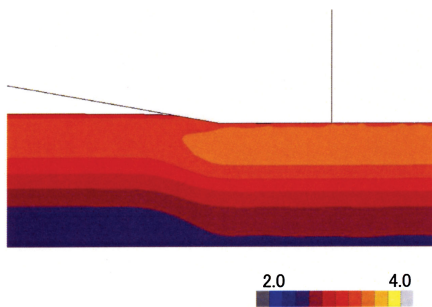


Fig. 15 Strain distribution in 15th stage of drawing

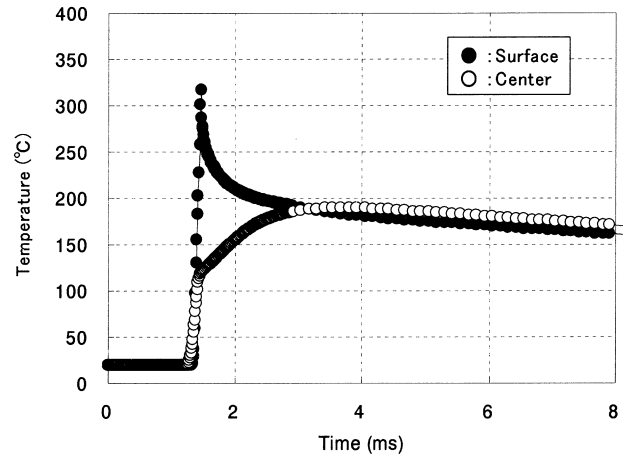


Fig. 16 Temperature history in 15th stage of drawing

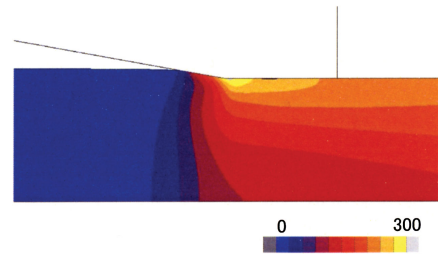


Fig. 17 Temperature distribution in 15th stage of drawing

The temperature of the land part on the material surface is high. The temperature measurement becomes increasingly difficult when there is an increase in material strength and a decrease in wire diameter. In this respect, the authors consider that the estimation of temperature by FEM analysis and the optimization of pass schedule based on temperature estimation will become important.

Since elastic-plastic FEM was applied to the present analysis of drawing, the authors consider applying the same FEM to estimate the residual stress after drawing. Although the present analysis is an example of axis-symmetric analysis, a general-purpose FEM program was used for the analysis. Therefore, the authors also consider applying the FEM to three-dimensional analysis of problems, such as the eccentricity during drawing.

References

- 1) Mori, K. et al.: J. Japan Soc. Technol. Plast. 46(536), 833(2005)
- 2) Toda, M. et al.: J. Japan Soc. Technol. Plast. 29(332), 971(1988)
- 3) Kada, O. et al.: Ann. CIRP, 47(1), 185(1998)
- 4) Terauchi, H.: Special Steel. 55(4), 21(2006)
- 5) Oyane, M.: J. Japan Soc. Technol. Plast. 13(135), 265(1972)
- 6) Pilarczyk, W. et al.: Wire Journal International. (Nov.), 76(1997)
- 7) Hamada, T. et al.: Wire Journal International. (May), 87(2001)
- 8) Kemp, L.P. et al.: Int. J. Mech. Sci. 27(11,12), 803(1985)
- 9) Komori, K.: J. Japan Soc. Technol. Plast. 39(452), 949(1989)